Quantum yield for N(^{4}S) production in the ultraviolet photolysis of N$_2$O

Tomoki Nakayama, Kenshi Takahashi, and Yutaka Matsumi

Solar-Terrestrial Environment Laboratory and Graduate School of Science, Nagoya University, Nagoya, Japan

Nori Taniguchi and Sachiko Hayashida

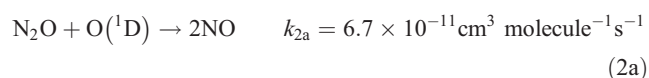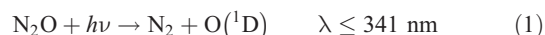Faculty of Science, Nara Women's University, Nara, Japan

[1] Direct detection of N(^{4}S) atom formation in the 193 nm photolysis of N$_2$O by a technique of vacuum ultraviolet (vuv) laser-induced fluorescence spectroscopy has been reported. Tunable vuv laser radiation around 120.071 nm that is resonant to the one-photon N(2p^{2}3s ^{4}P$_{1/2}$ − 2p^3 ^{4}S$_{3/2}$) transition has been generated by two-photon resonant four-wave sum frequency mixing in Hg vapor. The quantum yield value for N(^{4}S) formation in the N$_2$O photolysis at 193 nm has been determined to be 2.1 (±0.9) × 10^{-3}. The N(^{4}S) detection technique, which is developed in this study, is very sensitive, and the minimum detection limit is estimated to be 2 × 10^9 atoms cm^{-3}. Impact of the photolytic N(^{4}S) and NO(X^{2}Π) production from N$_2$O photolysis on stratospheric chemistry has been explored using a one-dimensional photochemical model, while the fragmentation was not considered in former model calculations. When the N(^{4}S) + NO dissociation channel is considered in the photochemical model, an enhancement of the NO$_x$ production rate (up to 3%) is observed, which is followed by a decrease of the steady state O$_3$ concentration throughout the stratosphere.   *INDEX TERMS:* 0317 Atmospheric Composition and Structure: Chemical kinetic and photochemical properties; 0340 Atmospheric Composition and Structure: Middle atmosphere—composition and chemistry; 0341 Atmospheric Composition and Structure: Middle atmosphere—constituent transport and chemistry (3334); *KEYWORDS:* N$_2$O photolysis, NO$_x$ production, stratosphere

Citation: Nakayama, T., K. Takahashi, Y. Matsumi, N. Taniguchi, and S. Hayashida, Quantum yield for N(^{4}S) production in the ultraviolet photolysis of N$_2$O, *J. Geophys. Res.*, *108*(D21), 4668, doi:10.1029/2003JD003709, 2003.
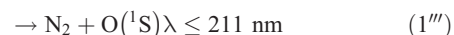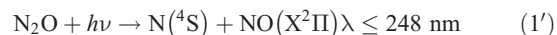
1. Introduction

[2] Nitrous oxide, N$_2$O, is an important atmospheric minor constituent as the main source of odd nitrogen (nitrogen compounds other than N$_2$) in the stratosphere. Not only do these nitrogen species catalytically destroy O$_3$ directly, but they also control the relative contributions of the ClO$_x$ and HO$_x$ cycles in the O$_3$ destruction in the stratosphere [*Brasseur et al.*, 1999]. Most of the N$_2$O transported through the planetary boundary layer and the free troposphere to the stratosphere is photolyzed at UV wavelengths to O(^{1}D) + N$_2$, while a small fraction of N$_2$O reacts with O(^{1}D) atoms.

$$N_2O + h\nu \rightarrow N_2 + O(^1D) \qquad \lambda \leq 341 \text{ nm} \qquad (1)$$

$$N_2O + O(^1D) \rightarrow 2NO \qquad k_{2a} = 6.7 \times 10^{-11} \text{cm}^3 \text{ molecule}^{-1}\text{s}^{-1} \qquad (2a)$$

$$\rightarrow N_2 + O_2, \qquad k_{2b} = 4.9 \times 10^{-11} \text{cm}^3 \text{ molecule}^{-1}\text{s}^{-1} \qquad (2b)$$

where the wavelength indicates the thermochemical threshold for channel (1), while k_{2a} and k_{2b} are the rate constants for reactions (2a) and (2b), respectively [*Sander et al.*, 2003].

[3] The N$_2$O photolysis around 200 nm has been considered to proceed through channel (1) with an almost unity quantum yield [*Okabe*, 1978] and the other energetically available channels are very minor:

$$N_2O + h\nu \rightarrow N(^4S) + NO(X^2\Pi)\lambda \leq 248 \text{ nm} \qquad (1')$$

$$\rightarrow N_2 + O(^3P)\lambda \leq 742 \text{ nm} \qquad (1'')$$

$$\rightarrow N_2 + O(^1S)\lambda \leq 211 \text{ nm} \qquad (1''')$$

Felder et al. [1991] studied the dissociation dynamics of N$_2$O at 193 nm by photofragments translational spectroscopy and reported that channel (1') was unimportant as the time-of-flight signal intensity at m/e = 30 was less than the detection limit. *Greenblatt and Ravishankara* [1990] reported the upper limit value of the quantum yield for channel (1') in the 193 nm photolysis of N$_2$O to be 8 × 10^{-3} through the chemiluminescent detection of NO products.

Recently, *Adams et al.* [2001] detected the N(^{4}S) formation in the 207 nm photolysis of N$_2$O by means of two-photon absorption laser-induced fluorescence technique (TALIF) using the same focused laser beam at 207 nm. They have not measured the quantum yield for N(^{4}S) formation. It is difficult to estimate the yield from the experiments using a one-color focused laser beam for both photolysis and probe.

[4] Although the oxidation of N$_2$O by O(^{1}D), channel (2a), is thought to be the dominant global source of NO in the stratosphere, the photodissociation reaction is a major removal process of stratospheric N$_2$O and the O(^{1}D) reaction is minor as stratospheric sink of N$_2$O. A simple calculation can predict that a quantum yield of 1% for channel (1′) in N$_2$O photolysis would represent an approximate increase of 15% in the active nitrogen production rate in the upper stratosphere. Therefore a precise determination of the channel (1′) quantum yield is essential for evaluating the stratospheric NO production rate.

[5] In this study, laboratory studies on the N(^{4}S) atom formation from the photolysis of N$_2$O at 193 nm has been carried out using a technique of laser-induced fluorescence in the vacuum ultraviolet region (vuv-LIF). The quantum yield for N(^{4}S) atom formation from N$_2$O photolysis at 193 nm is determined to be 2.1 (±0.9) × 10^{-3}. The atmospheric significance of channel (1′) as a new source of NO in the stratosphere has also been examined with a one-dimensional dynamical-photochemical model.

2. Experiment

[6] The experimental setup used in this study is similar to that in our previous studies [*Matsumi et al.*, 1994; *Hitsuda et al.*, 2001], and therefore only brief description is given here. The unpolarized output of an ArF excimer laser (Lambda Physik, COMPex 102) was employed as a photolysis laser to dissociate the N$_2$O parent molecules. The N(^{4}S) atoms produced from N$_2$O photolysis at 193 nm were probed by the vuv-LIF method at 120.071 nm, which is resonant with the electronic transition of N($2p^2 3s$ $^4P_{1/2}$ ← $2p^3$ $^4S_{3/2}$). The probe vuv laser radiation was generated by two-photon resonant four-wave sum frequency mixing ($\omega_{vuv} = 2\omega_1 + \omega_2$) in Hg vapor around 120.1 nm [*Hilbig and Wallenstein*, 1983]. Two dye lasers (Lambda Physik, Scanmate 2E and FL3002E) were simultaneously pumped by a XeCl excimer laser (Lambda Physik, COMPex 201). One dye laser operating with Rhodamine 101 dye in CH$_3$OH solvent generated 4−5 mJ pulse^{-1} around 625 nm. The visible output was frequency doubled in a KD*P crystal to obtain 312.76 nm (in air), which is two-photon resonant with the Hg electronic transition ($6s7s$ $^1S_0$ ← $6s^2$ $^1S_0$). The other dye laser operating with Coumarin 307 dye in CH$_3$OH solvent produced 2−4 mJ pulse^{-1} around 517 nm. The two laser beams were carefully overlapped using a dichroic mirror and focused into the Hg vapor cell with a fused silica lens (f = 250 mm). The temperature in the Hg vapor cell was controlled around 450−470 K to obtain enough vuv probe laser power for experiments, which corresponds to the equilibrium Hg vapor pressure of 8−14 Torr [*Smith and Alford*, 1987]. Kr was added in the Hg vapor cell for phase matching and the optimum partial pressure was 6−8 Torr. The generated vuv

laser light was introduced into a photolysis chamber through a LiF window that was used to separate the Hg vapor cell and the photolysis chamber. A fraction of the incident vuv light passed through the photolysis chamber was reflected by a thin LiF plate held in the end of the photolysis chamber and led into a nitric oxide (NO) photoionization cell. The relative intensity of vuv laser light was monitored by measuring the photoionization current. Typical NO gas pressure was 2−3 Torr.

[7] The vuv laser line width was estimated to be 0.28 cm^{-1} full width at half maximum (FWHM) with a Gaussian shape. The vuv laser line width was estimated from the shape of the Doppler profile of thermalized Cl($^2P_{1/2}$) atom, in which the Cl atoms were produced from HCl photolysis at 193 nm and were detected at 120.135 nm. The necessary vuv laser was generated with the same experimental setup as used for N atom detection. The Doppler profile was measured, when 2 Torr of Ar was added and the time delay between the photolysis and probe laser pulses was 20 μs. Under the experimental conditions, the translational energy of Cl atom is completely thermalized. The repetition rate of the photolysis and probe laser pulses was 10 Hz. The time delay between the photolysis and probe laser pulses was controlled by a digital delay generator (Stanford Research Systems, DG535). The typical time delay for N$_2$O photolysis experiments was 130 ns with a time jitter less than 20 ns.

[8] The vuv-LIF signals from the N(^{4}S) atoms were detected using a solar blind photomultiplier tube (PMT) (EMR, 542J-09-17). The PMT has an MgF$_2$ window and a KBr photocathode that is sensitive only between 115 and 165 nm. The observation direction of the LIF was perpendicular to both vuv probe and photolysis laser light, and perpendicular to the electric vector of the vuv probe laser. The output of the photomultiplier was preamplified and averaged over 10 laser pulses by a gated integrator (Stanford Research Systems, SR-250), and then stored on a personal computer.

[9] The photolysis chamber was made of stainless steel with the size 80 × 80 × 80 mm, and was continuously evacuated by a rotary pump (330 L min^{-1}) through a liquid N$_2$ trap. The total gas pressure in the chamber was measured by means of a Baratron gauge (MKS, 122A, 2 Torr full scale). N$_2$O (>99.9%) was supplied into the reaction chamber through a needle valve. The typical pressure of N$_2$O was 500−900 mTorr. While scanning the vuv laser wavelength for N(^{4}S) atom detections, the reactants pressure was kept constant. It should be noted that the high sensitivity of the vuv-LIF technique makes it possible to detect N(^{4}S) atoms at low gas pressures and short pump probe delay time (≤150 ns), and that chemical losses through secondary reactions, for example, N + N$_2$O, N + NO and N + O$_2$, can be safely ignored.

[10] In the titration experiments to calibrate the absolute sensitivity of the vuv-LIF system, N(^{4}S) atoms were generated by the microwave (2450 MHz) discharge of pure N$_2$ gas (>99.9%) in a flow tube (Pyrex, 13.7 mm i.d.). A coaxial flow tube was connected between the N$_2$ discharge flow tube and the vuv-LIF chamber. NO/Ar gas mixture (0.0268% of NO in Ar) was introduced through the inner injection tube (Pyrex, 3.8 mm i.d.), which can move along the outer flow tube. The gas flows were controlled by mass

flow controllers. All experiments in the present study were performed at room temperature.

3. Results

[11] Figure 1 shows the fluorescence excitation spectrum for N(^{4}S) atoms produced in the 193 nm photolysis of N$_2$O. The atomic line profiles of the N(^{4}P$_{1/2}$ ← ^{4}S$_{3/2}$) transition were directly observed by the vuv-LIF method around 120.071 nm. The dependence of the LIF signal intensity for the N(^{4}S) atoms on the photolysis laser pulse is shown in Figure 2. We also checked that no N(^{4}S) atoms signal was detected without 193 nm photolysis light. These results indicate that multiphoton absorption processes at 193 nm or dissociation of parent molecules by the probe laser beams (ω_{vuv}, ω_1, and ω_2) are safely ignored in this work. The quantum yield for N(^{4}S) formation from N$_2$O at 193 nm photolysis was determined by calibrating the sensitivity of the vuv-LIF system. The two methods were used to estimate the absolute sensitivity of the detection system for N(^{4}S) by the vuv-LIF method. One is the titration technique for the N(^{4}S) atom concentration using chemical reaction with NO. The other is the comparison between the LIF intensities of the N(^{4}S) atoms produced in the N$_2$O photolysis at 193 nm and Cl(^{2}P$_{1/2}$) atoms produced in the HCl photolysis at 193 nm. The Cl(^{2}P$_{1/2}$) quantum yield from the photolysis of HCl at 193 nm has already been reported [*Zhang et al.*, 1997].

3.1. Chemical Titration Method

[12] The conventional titration technique for N atoms was used to calibrate the vuv-LIF system for detecting N(^{4}S) atoms [*Boisse-Laporte et al.*, 1997]. The N(^{4}S) atoms were generated in a microwave (MW) discharge of pure N$_2$ gas and were then introduced into the vuv-LIF chamber through the coaxial flow tube. While monitoring the vuv-LIF signal
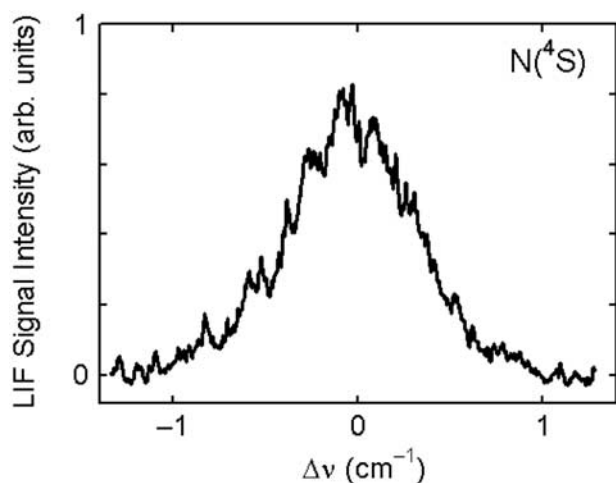

Figure 1. Fluorescence excitation spectra of N(^{4}S) produced from the photolysis of N$_2$O at 193 nm. The horizontal scale indicates the wave number shift from the resonance line center of the ^{4}P$_{1/2}$ ← ^{4}S$_{3/2}$ transition for N atom at 120.071 nm. The delay time between the photolysis and probe laser pulses was 130 ns. The pressure of N$_2$O was 700 mTorr.
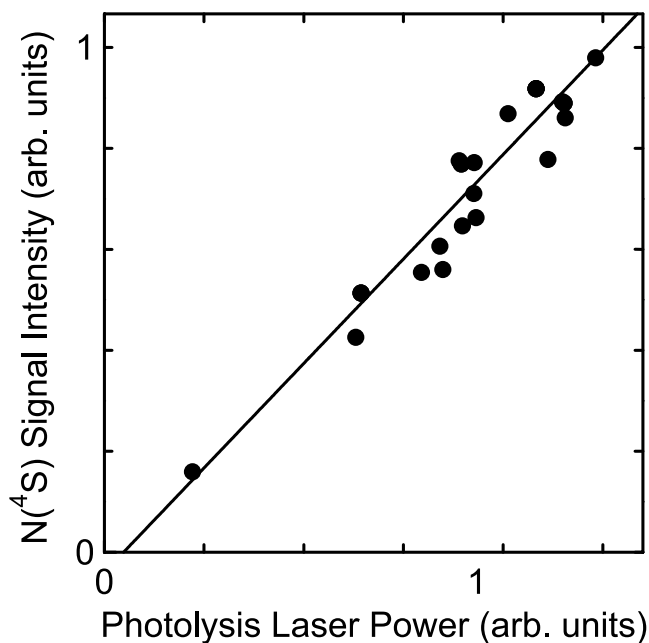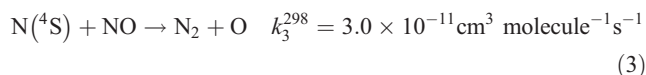

Figure 2. Plots of the LIF signal intensity of N(^{4}S) at 120.071 nm versus the photolysis laser power.

of N(^{4}S) atoms at 120.071 nm, NO molecules diluted with Ar were injected into the flow system. The N(^{4}S) atoms were consumed by the following reaction:

$$N(^4S) + NO \rightarrow N_2 + O \quad k_3^{298} = 3.0 \times 10^{-11} \text{cm}^3 \text{ molecule}^{-1}\text{s}^{-1} \tag{3}$$

where k_3^{298} is the rate constant for reaction (3) at 298 K [*Sander et al.*, 2003]. By monitoring the vuv-LIF signal intensities as a function of the number density of NO molecules added, the sensitivity of the vuv-LIF system for N atom detection was calibrated. A typical titration plot is shown in Figure 3, in which the mass flow rate of NO/Ar mixture was varied between 0.6 and 2.3 sccm while the total flow rate was kept constant (19 sccm). When all the N atoms produced by the MW discharge are consumed by reaction (3), the NO concentration corresponds to the initial N atom concentration. Thus the absolute concentration of N atoms detected by the vuv-LIF method was obtained. The inner NO injection tube is movable so that the reaction time can be varied by changing the location of the addition of the NO molecules. To check the wall reactivity of N(^{4}S), the titration experiments were carried out under different residence time conditions (0.2–0.5 s) by changing the location of the NO injection. No significant influence from the wall loss of N(^{4}S) atoms was observed, which is consistent with the very low wall reactivity reported by *Wennberg et al.* [1994].

[13] Fluorescence excitation spectra for N(^{4}S) atoms produced in the N$_2$O photolysis at 193 nm and the MW discharge of N$_2$ were measured to determine the quantum yield for N(^{4}S) formation in the N$_2$O photolysis. The N(^{4}S) production quantum yield from the photolysis of N$_2$O, Φ_N, is defined by the number density of N(^{4}S) atoms produced from the photolysis divided by the number density of N$_2$O
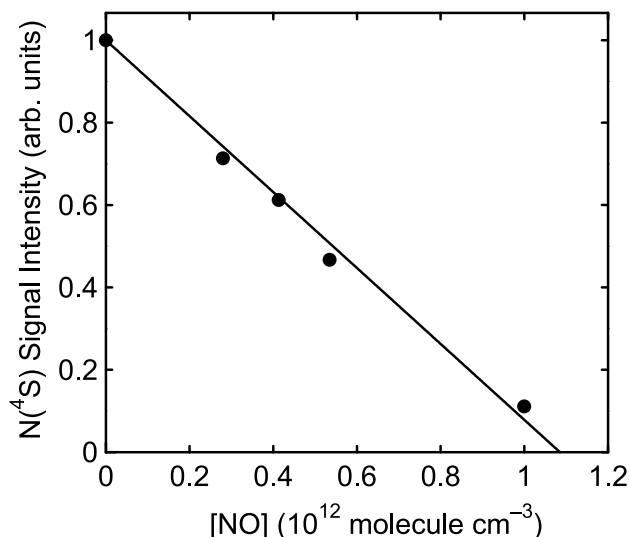
Figure 3. Plots of the titration for the N atoms produced by the microwave discharge of N$_2$. The horizontal axis is the NO concentration added downstream of the discharge. The vertical axis is the LIF intensity of N(^{4}S). The solid line indicates the results of the first-order least squares fitting.

molecules excited by the photolysis laser light at 193 nm, which is expressed as follows:

$$\Phi_N = \frac{(A_{Ph}/A_{MW})[N]_{MW}}{\sigma_{N2O}[N_2O]I_{Ph}} \times \frac{F_{MW}}{F_{Ph}} \qquad (4)$$

A_{Ph} and A_{MW} are the areas of the resonance peaks of the fluorescence excitation spectra of N(^{4}S) atoms produced in the photolysis of N$_2$O at 193 nm and in the MW discharge of N$_2$, respectively, under the same conditions for the N atom detection. $[N]_{MW}$ is the concentration of N atom produced in the MW discharge of N$_2$, which calibrated by the titration technique. σ_{N2O} is the photoabsorption cross section of N$_2$O at 193 nm, 8.95×10^{-20} cm^2 molecule^{-1} [*Sander et al.*, 2003]. $[N_2O]$ is the concentration of N$_2$O in the chamber. I_{Ph} is the photon density of the incident photolysis laser light, which was measured to be 8.4×10^{16} photons cm^{-2}. Intensity variation of the photolysis laser light was small (<5%) throughout the measurements. F_{Ph} and F_{MW} are the detection efficiencies of the fluorescence monitoring in the photolysis and MW discharge experiments, respectively, where the excitation volume by the probe vuv laser in the chamber, the overlap region of the 193 nm photolysis laser with the probe laser, and the solid angle from the emitting region onto the photocathode of the PMT are take into account. The length of the volume excited by the probe laser in the viewing zone of the PMT was 15 mm, while that of the volume where the probe laser beam overlapped with the photolysis laser was 6 mm. Therefore the value of F(MW)/F(ph) was estimated to be 2.5. Three sets of experiments were performed for the chemical titration method. Consequently, Φ_N was determined to be 2.25 ($\pm$0.71) $\times 10^{-3}$. The quoted error includes the 1σ statistical and estimated systematic uncertainties for

the vuv-LIF detection and the N atom concentration calibration.

3.2. Photolytic Calibration Method

[14] Cl(^{2}P$_{1/2}$) atoms produced from HCl photolysis at 193 nm were detected by the vuv-LIF technique at 120.135 nm, which is associated with electronic transition of Cl(3p^{4}4s ^{2}D$_{3/2}$ ← 3p^5 ^{2}P$_{1/2}$). The tunable vuv laser radiation around 120.135 nm was also obtained with the same experimental setup for the vuv laser system with the Hg vapor cell and the fluorescence detection system. Figure 4 shows the fluorescence excitation spectrum for Cl(^{2}P$_{1/2}$) atoms produced in the 193 nm photolysis of HCl. A gas mixture of HCl/Ar (12.3% of HCl in Ar) was used. By comparing the relative intensities of LIF signals of N(^{4}S) from N$_2$O and Cl(^{2}P$_{1/2}$) from HCl photolysis, the N(^{4}S) quantum yield can be estimated. Experimentally, measurements of spectra for N and Cl atom were alternatively performed by changing both the reactants and laser wavelengths.

[15] The quantum yield for N(^{4}S) formation, Φ_N, from the photolysis of N$_2$O at 193 nm is obtained by the following equation:

$$\Phi_N = \frac{A_N}{A_{Cl}} \frac{I_{Cl}}{I_N} \frac{\sigma_{HCl}}{\sigma_{N2O}} \frac{[HCl]}{[N_2O]} \frac{f_{Cl}}{f_N} \frac{\varphi_{Cl}}{\varphi_N} \Phi_{Cl} \qquad (5)$$

A_N and A_{Cl} are the areas of resonance peaks in the fluorescence excitation spectra of N(^{4}S) atoms in the photolysis of N$_2$O and Cl(^{2}P$_{1/2}$) atoms in the photolysis of HCl, respectively. I_N and I_{Cl} are the relative probe laser intensities for N and Cl atom detection which obtained as a photoionization current from the NO containing cell. The photoionization efficiencies of NO molecule used at 120.071 and 120.135 nm are also taken into account [*Ono et al.*, 1980; *Erman et al.*, 1995]. σ_{HCl} is the photoabsorption cross section of HCl at 193 nm, 8.69×10^{-20} cm^2 molecule^{-1} [*Sander et al.*, 2003]. [HCl] is the concentration of HCl molecules in the chamber. f_N and f_{Cl} are the oscillator strength values for the N(2p^{2}3s ^{4}P$_{1/2}$ ← 2p^3 ^{4}S$_{3/2}$) and Cl(3p^{4}4s ^{2}D$_{3/2}$ ← 3p^5 ^{2}P$_{1/2}$) optical excitation. The
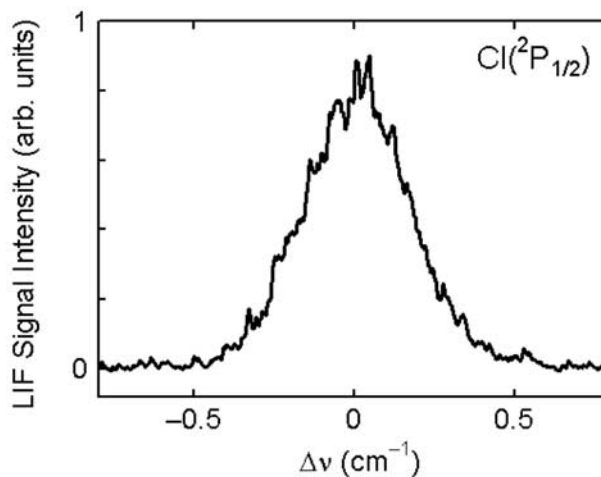

Figure 4. Fluorescence excitation spectra of Cl(^{2}P$_{1/2}$) atoms produced from the 193 nm photolysis of HCl.

values of f_N and f_{Cl} are taken from the database of *National Institute of Standards and Technology* [2003]. φ_N and φ_{Cl} indicate the detection efficiencies of the resonance fluorescence for N and Cl atoms, respectively. As for Cl($^2P_{1/2}$) atom detection, the excited Cl($^2D_{3/2}$) state fluoresces at 120.135 and 118.875 nm, which are resonant to the $^2D_{3/2} \rightarrow {}^2P_{1/2}$ and $^2D_{3/2} \rightarrow {}^2P_{3/2}$ transition, respectively. The detection efficiencies of the PMT system among the wavelengths at 120.071, 120.135 and 118.875 nm for the N($^4P_{1/2} \rightarrow {}^4S_{3/2}$), Cl($^2D_{3/2} \rightarrow {}^2P_{1/2}$) and Cl($^2D_{3/2} \rightarrow {}^2P_{3/2}$) emission lines, respectively, are assumed to be constant since those wavelength are very close. The quantum yield of Cl($^2P_{1/2}$) atoms in the photolysis of HCl at 193 nm photolysis, Φ_{Cl}, is reported to be 0.408 [*Zhang et al.*, 1997]. In this experiment, the collisional relaxation and the chemical reaction of Cl($^2P_{1/2}$) could be ignored. The pressures of HCl and Ar buffer gas were 20 and 160 mTorr and the time delay between the photolysis and probe laser pulses was 130 ns, and the relaxation rate of Cl($^2P_{1/2}$) by collision with HCl and Ar are 7.8×10^{-12} and $\leq 1.0 \times 10^{-14}$ cm^3 molecule^{-1} s^{-1}, respectively [*Hitsuda et al.*, 2001; *Sotnichenko et al.*, 1988]. Twenty-three sets of experiments were performed for photolytic calibration method. Consequently, $\Phi_N = 1.70 \ (\pm 1.21) \times 10^{-3}$ was obtained. The quoted error includes the 1σ statistical and estimated systematic uncertainties.

[16] The results obtained from the two different experiments of the chemical titration and photolytic calibration methods are in good agreement with each other within the experimental uncertainties. The quantum yield value for N(^{4}S) formation in the 193 nm photolysis of N$_2$O is determined to be $\Phi_N = 2.1 \ (\pm 0.9) \times 10^{-3}$ by combining the experiments results from two methods, in which the majority of the error from each of the two methods are systematic uncertainties.

4. Discussion

4.1. Dissociation Process of N$_2$O to Produce N(^{4}S) + NO

[17] In the photolysis of N$_2$O around 200 nm, there are four energetically available dissociation pathways (1)–(1‴). In this work, we determined the quantum yield for N(^{4}S) production in the photolysis of N$_2$O at 193 nm. Our result of $\Phi_N = 2.1 \ (\pm 0.9) \times 10^{-3}$ is smaller than the upper limit value presented by *Greenblatt and Ravishankara* [1990]. They estimated the NO production yield (channel (1′)) by observing the chemiluminescence of NO$_2$ that was formed by the reaction of O$_3$ and NO fragments produced from N$_2$O photolysis. A quite small quantum yield value can be explained by a spin-forbidden nature for channel (1′).

[18] Figure 5 shows the correlation diagram for the reactions of O + N$_2$ and NO + N, in which C_s symmetry is assumed for the reaction intermediate [*Hopper*, 1984]. N$_2$O has 16 valence electrons and belongs to $C_{\infty v}$ symmetry group when it is in its electronic ground state X $^1\Sigma^+$ ($4\sigma^2 5\sigma^2 6\sigma^2 1\pi^4 7\sigma^2 2\pi^4$ configuration). The lowest electronically exited singlet states are the A $^1\Sigma^-$, the B $^1\Delta$, and the C $^1\Pi$ states. Upon bending the C_s symmetry group applies giving rise to the 1 ^{1}A′ ($^1\Sigma^+$) and the 1 ^{1}A″ ($^1\Sigma^-$) states. The Π and Δ states split into A′ and A″ components. The theoretical calculations by *Hopper* [1984] show that disso-
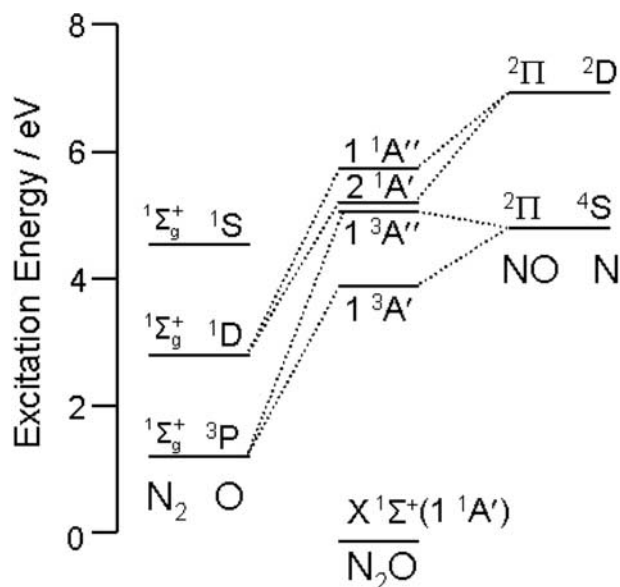
Figure 5. Adiabatic correlation diagram for N$_2$O (N-NO, N$_2$O, and N$_2$-O) system assuming a C_s symmetry, which is taken from *Hopper* [1984]. The energy levels are drawn to scale.

ciation around 200 nm occurs via the 2 ^{1}A′ state, and that the nearby 1 ^{1}A″ state can also be involved in the dissociation process. While the 2 ^{1}A′ state is part of a Renner-Teller pair, the component of this pair has a linear equilibrium geometry and its energy increases rapidly as the molecule bends. *Teule et al.* [2000] studied the photodissociation of N$_2$O around 203 nm by a technique of photofragment imaging, and showed that the parallel transition to the 2 ^{1}A′ state is dominant.

[19] Previous studies showed that channel (1) is dominant with almost unity quantum yield in the 193 nm photolysis of N$_2$O [*Okabe*, 1978], which is rationalized by the fact that both the 2 ^{1}A′ and 1 ^{1}A″ states adiabatically correlate to the photoproducts of O(^{1}D) + N$_2$ (channel (1)). In the present study, the N(^{4}S) atom formation (channel (1′)) is observed directly by the vuv-LIF method and the quantum yield is determined to be $2.1 \ (\pm 0.9) \times 10^{-3}$. The adiabatic correlation diagram shown in Figure 5 suggests that the intersystem crossing from the excited singlet state to the triplet state or direct photoexcitation to the triplet states can account for the N(^{4}S) formation. A weak spin-orbit interaction between the singlet and triplet excited states or a small transition probability from the ground to the triplet states may results in the very small quantum yield for N(^{4}S) formation in N$_2$O photolysis at 193 nm.
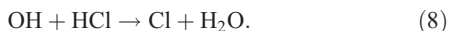
4.2. Atmospheric Implications

[20] We have investigated the atmospheric importance of channel (1′). A gap between the Shumann-Runge band of O$_2$ and the Hartley band of O$_3$ allows far ultraviolet solar radiation to reach the stratosphere. The wavelength region around 200 nm is known as "atmospheric window" in the stratosphere. The stratospheric sink of N$_2$O is mainly due to UV photolysis in the atmospheric window region. The remaining sink of N$_2$O is reaction with O(^{1}D) which is produced by the ozone photolysis.

Reaction (2a) is an important source of stratospheric NO. The photolysis of N$_2$O proceeding via photodissociation channel N(^{4}S) + NO can also provide a stratospheric NO source.

[21] The current NASA/JPL evaluation [*Sander et al.*, 2003] for stratospheric modeling recommends that the quantum yield for photodissociation of N$_2$O around 200 nm is unity, and the products are N$_2$ and O(^{1}D) (channel (1)). However, the N(^{4}S) and NO($^2\Pi$) formation (channel (1$'$)) can be a nonnegligible direct source of stratospheric NO$_x$ (= N + NO + NO$_2$). The stratospheric O$_3$ abundance and its vertical profile are significantly affected by NO$_x$, because NO$_x$ can catalytically destroy stratospheric O$_3$. In this study, we have investigated the atmospheric importance of channel (1$'$) in the photolysis of N$_2$O, by using a one-dimensional dynamical-photochemical model. All chemical schemes of the model are the same with that in the Garcia-Solomon two-dimensional (GS-2D) model [*Solomon et al.*, 1996]. The model calculations were performed including 40 chemical species and 120 chemical reactions with the chemical kinetics and photochemical data presented by the recent JPL recommendations [*Sander et al.*, 2003]. We included channel (1$'$) quantum yield value of 2.1 × 10^{-3} in the model on the assumption that it is independent of the temperature and wavelength at the atmospheric window region.

[22] Figure 6 shows the result of the photochemical model calculations for latitude of 40° in March, which indicates the change in the diurnally averaged concentrations of NO$_x$, HO$_x$ (= H + OH + HO$_2$), ClO$_x$ (= Cl + ClO) and O$_3$ calculated with or without channel (1$'$) in the photolysis of N$_2$O. The steady state NO$_x$ concentration calculated by the model including channel (1$'$) increases up to ~3% around 25 km in comparison with that ignoring channel (1$'$), while the HO$_x$ and ClO$_x$ abundances decrease. The altitude-dependent change in the NO$_x$ concentration should reflect the altitude-dependent solar flux at the atmospheric window wavelength region. The perturbations in the concentrations of HO$_x$ and ClO$_x$ may be attributable to the following reactions:

$$OH + NO_2 + M \rightarrow HNO_3 + M \qquad (6)$$

$$ClO + NO_2 + M \rightarrow ClONO_2 + M \qquad (7)$$

$$OH + HCl \rightarrow Cl + H_2O. \qquad (8)$$

The concentration changes of HO$_x$ and ClO$_x$ are larger in the lower stratosphere as shown in Figure 6, because the contribution of three-body reactions (6) and (7) becomes more significant at lower stratospheric altitudes. Reaction (8) converts the chlorine reservoir HCl into active ClO$_x$. The decrease of the HO$_x$ concentration may result in the decrease of ClO$_x$ through reaction (8). The chemical reactions of NO$_x$, HO$_x$ and ClO$_x$ families play a crucial role in determining the stratospheric O$_3$ abundance, and thus the concentration changes of these species alter O$_3$ abundance. Inclusion of channel (1$'$) in the model affects the production rate of NO$_x$, which is followed by the decrease of O$_3$ abundance through the
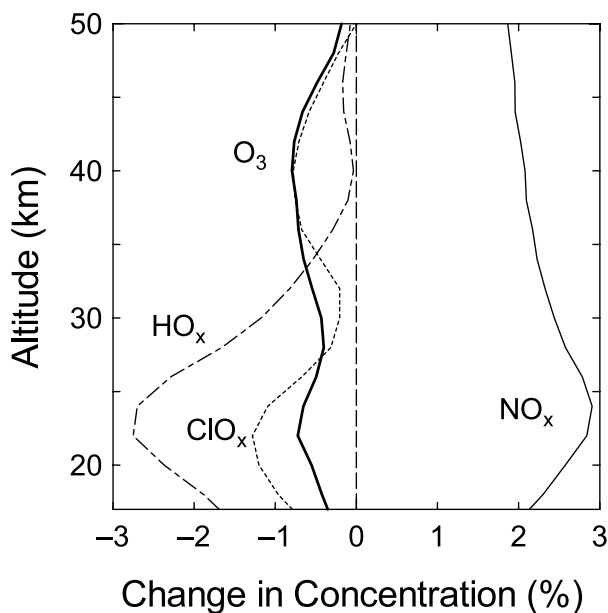

Figure 6. Calculated percentage changes in NO$_x$, HO$_x$, ClO$_x$, and O$_3$ concentrations with the N(^{4}S) + NO dissociation channel from those calculated without the N(^{4}S) + NO channel for latitude of 40° in March as a function of altitude.

enhancement of the NO$_x$ catalyzed O$_3$ destruction rate, as shown in Figure 6.

[23] The chemical reactions involving the nitrogen atoms play a crucial role in the Earth's and planetaries' atmospheres [*Yung and DeMore*, 1999]. For example, the reaction of N(^{4}S) with O$_2$ can be an important NO source in the Earth's lower thermosphere, where the N(^{4}S) atoms are produced by the solar vacuum and extreme ultraviolet photolysis of NO molecules [*Dothe et al.*, 1997]. In the Titan's atmosphere, the reactions of N(^{4}S) atoms with hydrocarbons are important as a source of highly reactive CN radicals. Therefore it is essential for understanding the terrestrial atmospheric processes to study the chemical reactions of nitrogen atoms. In this study, the ground state nitrogen atom, N(^{4}S), was detected directly by the laser-induced fluorescence technique at 120.071 nm. N(^{4}S) atom was produced in the photolysis of N$_2$O at 193 nm or microwave discharge of N$_2$. This is the first report of the vuv-LIF detection of N(^{4}S) atom as far as we have searched. The minimum detection limit is estimated to be 2 × 10^9 atoms cm^{-3} under our experimental conditions. The pulsed photodissociation of N$_2$O molecules and high-sensitivity detection technique for N(^{4}S) atom are applicable to the studies of the kinetics and dynamics of the chemical reaction processes involving N(^{4}S) atoms.

References

Adams, S. F., C. A. DeJoseph Jr., C. C. Carter, T. A. Miller, and J. M. Williamson, Kinetics of atomic nitrogen photofragment produced by laser photodissociation of N$_2$O, *J. Phys. Chem. A*, *105*, 5977–5983, 2001.

Boisse-Laporte, C., C. Chave-Normand, and J. Marec, A microwave plasma source of neutral nitrogen atoms, *Plasma Sources Sci. Technol.*, *6*, 70–77, 1997.

Brasseur, G. P., J. J. Orlando, and G. S. Tyndall, *Atmospheric Chemistry and Global Change*, Oxford Univ. Press, New York, 1999.

Dothe, H., R. D. Sharma, and J. W. Duff, On the steady-state assumption for the energy distribution function of the nonthermal N(^{4}S) atoms and the efficiency of NO production by these atoms in the terrestrial thermosphere, *Geophys. Res. Lett.*, *24*, 3233–3236, 1997.

Erman, P., A. Karawajczyk, E. Rachlew-Källne, and C. Strömholm, Photoionization and photodissociation of nitric oxide in the range 9–35eV, *J. Chem. Phys.*, *102*, 3064–3076, 1995.

Felder, P., B.-M. Haas, and J. R. Huber, The photoreaction N$_2$O $\rightarrow$ O(^{1}D) + N$_2$($^1\Sigma$) at 193 nm studied by photofragment translational spectroscopy, *Chem. Phys. Lett.*, *186*, 177–182, 1991.

Greenblatt, G. D., and A. R. Ravishankara, Laboratory studies on the stratospheric NO$_x$ production rate, *J. Geophys. Res.*, *95*, 3539–3547, 1990.

Hilbig, R., and R. Wallenstein, Resonant sum and difference frequency mixing in Hg, *IEEE J. Quantum Electron.*, *19*, 1759–1770, 1983.

Hitsuda, K., K. Takahashi, Y. Matsumi, and T. J. Wallington, Kinetics of the reactions of Cl(^{2}P$_{1/2}$) and Cl(^{2}P$_{3/2}$) atoms with C$_2$H$_6$, C$_2$D$_6$, CH$_3$F, C$_2$H$_5$F, and CH$_3$CF$_3$ at 298 K, *J. Phys. Chem. A*, *105*, 5131–5136, 2001.

Hopper, D. G., Ab initio multiple root optimization MCSCF study of the C$_{\infty v}$/C$_s$ excitation spectra and potential energy surfaces of N$_2$O, *J. Chem. Phys.*, *80*, 4290–4316, 1984.

Matsumi, Y., S. M. Shamsuddin, Y. Sato, and M. Kawasaki, Velocity relaxation of hot O(^{1}D) atoms by collisions with rare gases, N$_2$, and O$_2$, *J. Chem. Phys.*, *101*, 9610–9618, 1994.

National Institute of Standards and Technology, Atomic and Molecular Physics, in NIST Scientific and Technical Databases, http://www.nist.gov/srd/atomic.htm, Gaithersburg, Md., 2003.

Okabe, H., *Photochemistry of Small Molecules*, John Wiley, Hoboken, N. J., 1978.

Ono, Y., S. H. Linn, H. F. Prest, and C. Y. Ng, Higher resolution photoionization study of NO near the threshold, *J. Chem. Phys.*, *73*, 4855–4861, 1980.

Sander, S. P., et al., Chemical kinetics and photochemical data for use in atmospheric studies, *Publ. 02-25*, Jet Propul. Lab., Pasadena, Calif., 2003.

Smith, A. V., and W. J. Alford, Practical guide for 7S resonant frequency mixing in mercury: Generation of light in the 230–185- and 140–120-nm ranges, *J. Opt. Soc. Am. B*, *4*, 1765–1770, 1987.

Solomon, S., R. W. Portmann, R. R. Garcia, L. W. Thomason, L. R. Poole, and M. P. McCormick, The role of aerosol variations in anthropogenic ozone depletion at northern midlatitudes, *J. Geophys. Res.*, *101*, 6713–6727, 1996.

Sotnichenko, S. A., V. C. Bokun, and A. I. Nadkhin, Collisional quenching of chlorine (3 ^{2}P$_{1/2}$) by H$_2$, D$_2$, CO, O$_2$, N$_2$, and CO$_2$, *Chem. Phys. Lett.*, *153*, 560–568, 1988.

Teule, J. M., G. C. Groenenboom, D. W. Neyer, D. W. Chandler, and M. H. M. Janssen, State-to-state photodynamics of nitrous oxide and the effect of long-range interaction on the alignment of O(^{1}D$_2$), *Chem. Phys. Lett.*, *320*, 177–185, 2000.

Wennberg, P. O., J. G. Anderson, and D. K. Weisenstein, Kinetics of reactions of ground state nitrogen atoms (^{4}S$_{3/2}$) with NO and NO$_2$, *J. Geophys. Res.*, *99*, 18,839–18,846, 1994.

Yung, Y. L., and W. B. DeMore, *Photochemistry of Planetary Atmospheres*, Oxford Univ. Press, New York, 1999.

Zhang, J., M. Dulligan, and C. Wittig, Photodissociation of HCl at 193. 3 nm: Spin-orbit branching ratio, *J. Chem. Phys.*, *107*, 1403–1405, 1997.

———————————

Y. Matsumi, T. Nakayama, and K. Takahashi, Solar-Terrestrial Environment Laboratory and Graduate School of Science, Nagoya University, Honohara 3-13, Toyokawa, Aichi, 442-8507, Japan. (matsumi@stelab.nagoya-u.ac.jp; nakayama@stelab.nagoya-u.ac.jp; kent@stelab.nagoya-u.ac.jp)

S. Hayashida and N. Taniguchi, Faculty of Science, Nara Women's University, Kitauoya-Nishimachi, Nara, 630-8506, Japan. (sachiko@ics.nara-wu.ac.jp; ntanig@ics.nara-wu.ac.jp)